nature astronomy

REVIEW ARTICLE

DOI: 10.1038/s41550-017-0257-3

The Pluto system after the New Horizons flyby

Catherine B. Olkin[1]*, Kimberly Ennico[2] and John Spencer[1]

In July 2015, NASA's New Horizons mission performed a flyby of Pluto, revealing details about the geology, surface composition and atmospheres of this world and its moons that are unobtainable from Earth. With a resolution as small as 80 metres per pixel, New Horizons' images identified a large number of surface features, including a large basin filled with glacial ices that appear to be undergoing convection. Maps of surface composition show latitudinal banding, with non-volatile material dominating the equatorial region and volatile ices at mid- and polar latitudes. This pattern is driven by the seasonal cycle of solar insolation. New Horizons' atmospheric investigation found the temperature of Pluto's upper atmosphere to be much cooler than previously modelled. Images of forward-scattered sunlight revealed numerous haze layers extending up to 200 km from the surface. These discoveries have transformed our understanding of icy worlds in the outer Solar System, demonstrating that even at great distances from the Sun, worlds can have active geologic processes. This Review addresses our current understanding of the Pluto system and places it in context with previous investigations.

Before the July 2015 flyby of New Horizons through the Pluto system, astronomers had little information about the surface appearance of Pluto and its largest moon Charon. They knew that Pluto was redder (and getting redder with time) and had a higher albedo than Charon[1–3], and also had a bright polar cap[4] and a dark equatorial band[5]. There was considerable uncertainty about Pluto's exact size: estimates of its radius ranged from 1,151 km to 1,178 km (refs [6,7]). Charon's diameter was estimated to be approximately half that of Pluto's, and there was considerable uncertainty regarding the size of Pluto's small moons. Figure 1 shows some key milestones in the quest to obtain ever-better spatial imagery of these far-away worlds.

Light curves to maps

The small angular sizes of Pluto and Charon — 0.1 arcseconds and 0.05 arcseconds at perihelion, respectively (in 1989) — makes it difficult to map their surfaces using ground-based telescopes (Box 1). The first surface 'maps' were constructed by indirect light-curve inversion techniques thanks to observations of mutual transit and occultation events of Pluto and Charon[8–11], and this was followed by direct mapping using the Hubble Space Telescope (HST)[3,12,13]. These maps had only a few resolution elements across Pluto's disk. Combined with hemispheric-composition data from ground-based spectra (see 'Compositional complexity in the Pluto system'), they formed the basis for choosing the New Horizons Pluto flyby encounter hemisphere (the face observed at closest approach) and multi-instrument observation sequence[14]. From seven days before closest approach until two days after, the New Horizons instrument suite made more than 400 different observations of Pluto and its moons.

Pluto and Charon emerge as geological worlds

Several months before the July 2015 flyby, New Horizons began to obtain imagery better than the 1994 HST Faint Object Camera images, and each following day revealed new details. With weeks to go before closest approach, it was already clear that Pluto had a more complex geology than previously predicted.

Because Pluto and Charon rotate synchronously about a common centre of gravity every 6.4 Earth days, New Horizons imagery in the last week before closest approach provided a map of all the illuminated surfaces of both bodies (Fig. 2). With some exceptions, terrain below 38° S latitude was not viewable by New Horizons because it was unilluminated as a result of the northern summer season. From the New Horizons data, we know that Pluto's range of surface reflectance is extreme, varying in the range of 0.08–1.0, whereas Charon exhibits less variability across its surface[15].

Pluto. Much of Pluto's encounter hemisphere is moderately to heavily cratered, and is thus likely to have its origins early in the Solar System's history[16]. The size distribution of impact craters on both Pluto and Charon, when translated into impactor size, is roughly consistent with the observed size distribution of equivalent-sized Kuiper Belt objects, but reveals a surprising lack of impactors smaller than 1–2 km in diameter. The ancient terrain is cut by a sparse network of extensional faults, likely due to global expansion resulting from partial freezing of an internal ocean[16], or phase changes in the ice shell[17]. However, many areas of Pluto are much younger. Large regions, particularly the north polar region, are partially covered in deposits of material — several kilometres thick — that have been locally eroded to reveal the older terrain beneath[18]. The composition, origin and removal method of these deposits remains a mystery. Surface textures in some areas, which resemble 'penitentes' formed by sublimation of terrestrial snowfields, but on a scale 1,000 times larger, suggest that sublimation, perhaps of methane, has been an important erosional process[16].

The dominant geological feature on Pluto's encounter hemisphere is a large 750 km × 1,400 km depression, 3–4 km deep, called Sputnik Planitia (SP)[16,19]. (Note that all names of surface features on Pluto and its moons are currently informal.) The floor of SP, which is extremely flat, is composed of bright N_2, CH_4 and CO ices (details below). From the lack of resolvable impact craters, this surface is geologically young (<10 Myr ago)[16]. This ice surface is clearly mobile: there are obvious flow features near the margins, and much of SP is occupied by polygonal features that appear to be active convection cells[16,20,21]. Computational models that assume the rheological properties of solid N_2 and only present-day radiogenic heating predict resurfacing times of ~0.5 Myr, which is in agreement with the lack of impact craters. It is likely that SP occupies an ancient impact basin[16,19], although it is also possible that the weight of the ice itself created the depression[22]. The location of SP, close to

[1]Southwest Research Institute, Boulder, CO 80302, USA. [2]NASA Ames Research Center, Moffett Field, CA 94035, USA. *e-mail: colkin@boulder.swri.edu

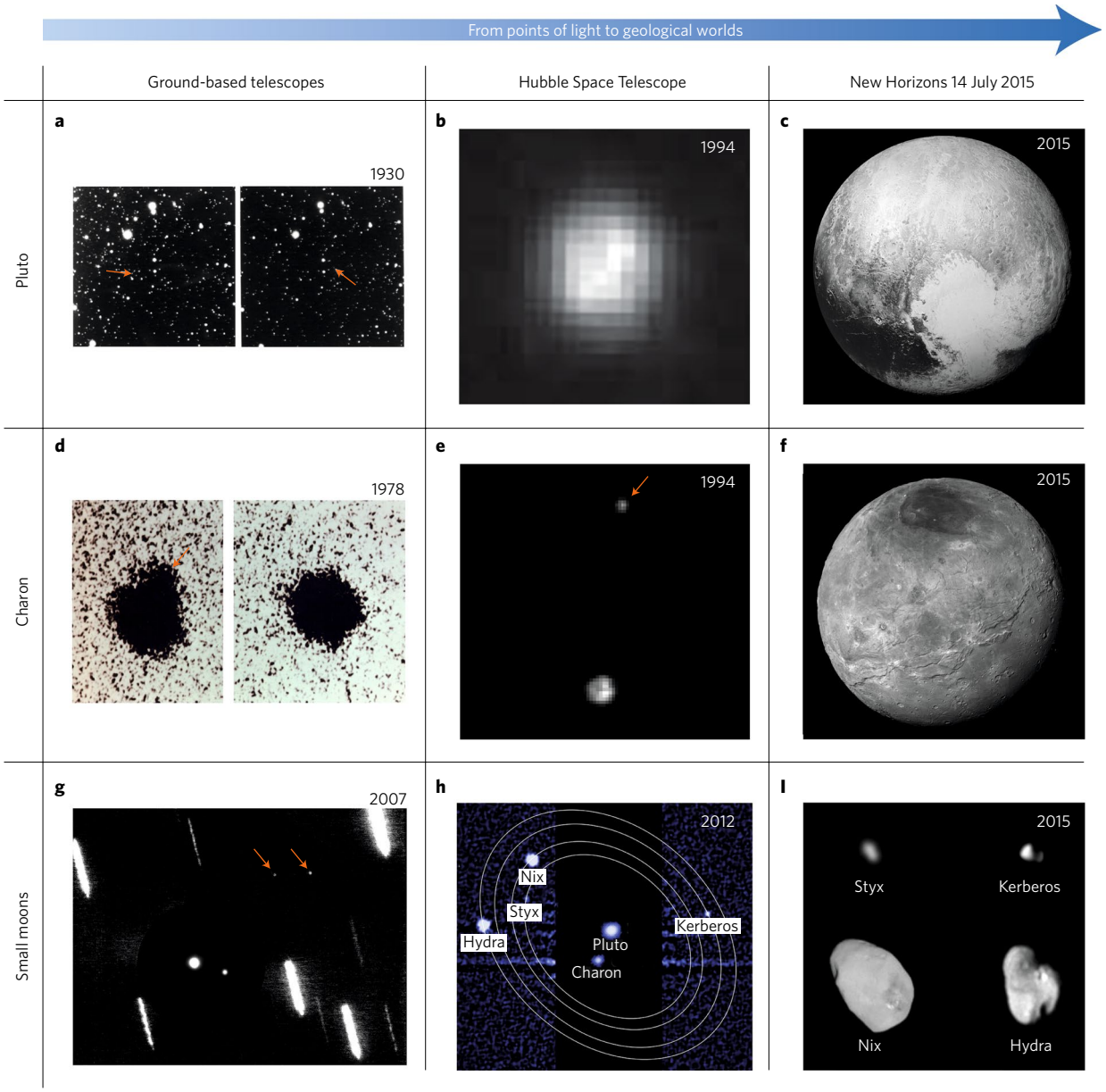

Fig. 1 | The Pluto system as seen through the years with increasing technical capabilities. a, Pluto discovery images. **b**, Pluto as imaged by the HST Faint Object Camera in 1994 (200 m pixel^{-1}). **c**, Pluto imaged by the New Horizons' high-resolution camera from a distance of ~450,000 km (2.2 km pixel^{-1}). **d**, Charon discovery image. The moon is seen in the left image (indicated by the arrow) but absent in the right image. **e**, Charon (top) and Pluto (bottom), separated by less than 1 arcsec, as observed by the HST in 1994. **f**, Charon imaged by New Horizons from a distance of ~174,000 km (~860 m pixel^{-1}). **g**, The two brightest small moons of Pluto: Nix (left arrow) and Hydra (right arrow), as observed by Keck using adaptive optics. The streaks are star trails. **h**, The Pluto system as imaged by the HST, indicating the orbits of the four small moons. **i**, New Horizons images of the four smaller moons: Styx (3.1 km pixel^{-1}), Nix (300 m pixel^{-1}), Kerberos (1.97 km pixel^{-1}) and Hydra (1.14 km pixel^{-1}). Credits: **a**, Lowell Observatory Archives; **b**–**d**, NASA/JHUAPL/SwRI; **e**, ESA; **f**, NASA; **g**, David Tholen; **h**, STScI; **i**, adapted from ref. 62, AAAS.

the anti-Charon point on Pluto (Fig. 2), is consistent with it being a positive mass anomaly that would be stable at this location due to tidal torques from Charon. This mass concentration might be explained if the thinner crust expected under a large impact basin allowed a denser liquid-water ocean underlying Pluto's ice shell to reach closer to the surface at this location[19,23] (Fig. 3), thus providing indirect evidence for such an ocean. New Horizons could not detect gravitational anomalies because the mass signature was small at the flyby distance.

The highland terrains to the north and east of SP feature extensive erosional features such as dendritic valley networks, which probably result from former glacial activity. There are also currently active glaciers, likely also dominated by N_2, which flow down into SP from the east[18,20]. The western margin of SP features very different landforms: chaotic regions of jumbled mountain-sized water ice blocks reaching 5 km in height[16]. Because water ice is less dense than the nitrogen-dominated ices of SP that surround many of these mountains, they may be literally floating like icebergs in SP, and may have been transported to their current locations by the movement of the mobile nitrogen ice. To the southwest of SP are two large mountains with central depressions (informally called Wright Mons and Piccard Mons), which may be cryovolcanic constructs[16]. These are also lightly cratered, and thus geologically recent.

Box 1 | From points of light to geological worlds

Data from New Horizons provided significant leaps in spatial resolution over earlier HST and ground-based images (Fig. 1). Clyde Tombaugh at Lowell Observatory in Flagstaff, Arizona, discovered Pluto in early 1930 after over nearly a year of searching, using a 32.5 cm telescope and recording images on photographic plates[56]. He used a blink comparator, an instrument that rapidly shifted back and forth between views of each of the plates, to reveal the movement of any object that had changed position or appearance between photographs. Decades later, with the launch of the HST, observations of Pluto with a resolution of around 200 km pixel^{-1} were obtained by the HST's Faint Object Camera in 1994[13]. Although the image was too coarse to provide information on Pluto's surface geology, it confirmed significant albedo differences across the surface, as previously inferred from the mutual event observations in the 1980s. Subsequent HST imagery of Pluto taken in 2002–2003 showed its brightness had changed, with its north pole getting brighter and its southern regions getting redder and darker[3]. Images from New Horizons transformed our understanding of Pluto from an astronomer's world to a geologic one, with spatial resolutions in selected areas as small as 80 m pixel^{-1}. The closest-approach hemisphere is rich in geological diversity, with the most prominent feature being a heart-shaped bright region, the western half of which is a basin filled with nitrogen, methane and carbon monoxide ices, superimposed on a dark equatorial band. The New Horizons images also provided a means of determining Pluto's size. The mean radius of Pluto is 1,188 ± 1.6 km (ref. [23]) and there is no evidence of distortion.

Charon, Pluto's largest moon, was discovered in 1978 by Christy and Harrington using the 1.55 m telescope at the US Naval Observatory Flagstaff Station[57,58]. The images showed a slight elongation in Pluto's appearance, which occurred periodically with an ~6.4 day cadence — the same as Pluto's rotational period. This elongation was eventually understood to be a moon (Charon) in orbit around Pluto. With less than 1 arcsec separation, resolving Pluto and Charon was challenging, but has since become more routine using 8 m ground-based facilities with adaptive optics, and high-angular-resolution submillimetre facilities such as the Atacama Large Millimeter/submillimeter Array and the HST. The New Horizons images transformed our understanding of Charon, just as they did for Pluto. The most prominent features on Charon's closest-approach hemisphere are a dark red polar region and a tectonic belt that splits Charon's visible surface geology into two distinct hemispheres: a relatively smooth region in the south, and a more rugged terrain in the north[26].

The four smaller moons of Pluto were discovered using HST: Nix and Hydra in 2005[59], Kerberos in 2011[60] and Styx in 2012[61]. After their discovery, it was possible using adaptive optics from the 10 m Keck Observatory to image Nix and Hydra, the larger of Pluto's small moons. This is remarkable given their distance from Earth (~33 au) and small size (50 km × 35 km × 33 km for Nix and 65 km × 45 km × 25 km for Hydra[62]). New Horizons images of all four smaller moons reveal elongated shapes and brighter-than-expected reflectances. Infrared spectra taken by New Horizons confirmed the interpretation that the bright surfaces of these objects are due primarily to water ice. The surfaces of Nix and Hydra exhibit features that are consistent with impact craters, with 11 craters identified on Nix[62].

Pluto therefore displays a remarkable variety of geological processes, some of which continue to be active. Such complex and youthful activity was unexpected because Pluto experiences none of the tidal heating thought to power geological activity on many ice satellites. The most likely explanation is that Pluto's feeble supply of radiogenic heat is sufficient to power geological activity owing to the presence of volatile ices in its interior. Nevertheless, Pluto's surface is in general much older than that of Triton, Neptune's largest moon[24], which is similar in size, density and surface composition to Pluto. Pluto's more rugged topography also suggests its ice shell is thicker and colder than that of Triton. This difference may provide evidence that Triton has an additional, probably tidal, heat source[25].

Charon. Charon also surprised us with the discovery of its red polar region, which had not been predicted by ground-based observations, and its circumequatorial tectonic belt, which separates distinctive northern (more rugged, cratered) and southern (smoother) plains[26]. Elevation extremes appear to be ~10 km and are made possible by the strength of Charon's dominant surface component (water ice) combined with its modest surface gravity. Charon's crater counts indicate its surface overall is quite ancient (~4 Gyr ago)[27].

Charon exhibits intriguing geological features not seen on Pluto, such as sunken mountains[28] and landslides. The sunken mountains could be the result of flexure in Charon's lithosphere or the flow of viscous cryovolcanic materials.

The many extensional features (for example, chasms, faults and rifts) of Charon suggest it was once slightly smaller and may have undergone a transition that increased its radius. The freezing of an internal ocean could have driven this expansion and would be consistent with its nearly spherical shape[23]. However, models of the freezing and expansion[29] do not explain the north–south dichotomy in topography.

Compositional complexity in the Pluto system

Before the New Horizons flyby, Earth-based investigations of the composition of Pluto and Charon had revealed only limited information about the spatial resolution of compositional units. The surface of Pluto was known to have volatile ices such as nitrogen (N_2), methane (CH_4), carbon monoxide (CO) and ethane (C_2H_6) (ref. [30]). Intriguingly, the CO was located primarily on the anti-Charon face of Pluto, and this was one factor in choosing the anti-Charon face of Pluto for the encounter hemisphere at closest approach[14]. At the surface temperature and pressure of Pluto, N_2, CH_4 and CO are volatile and can be transported via sublimation and condensation. The main driver of the atmospheric pressure on Pluto is the temperature of the most volatile ice (N_2), which changes seasonally with insolation. At Pluto's surface temperatures (~40 K), pure CH_4 ice does not coexist with pure N_2 ice; instead they form solid solutions[31]. It is also likely that Pluto's CO is in solid solution with its other volatile ices.

Pluto. Composition maps of Pluto's surface have been produced from New Horizons data using three different methods: (1) equivalent widths of selected features[32]; (2) modelling of the bidirectional reflectance[33]; and (3) principal component analysis[34]. All three methods yield the same broad results: SP is a vast reservoir of volatile ices (N_2, CH_4 and CO), and outside SP there is a general latitudinal dependence of tholin composition (red material resulting from the irradiation of hydrocarbons)[35] near the equator, N_2 ice at mid-latitudes, and CH_4 ice north of ~60° (Fig. 4).

A number of models have demonstrated that volatile ices are stable in SP over long timescales. Modelling the insolation on surface elements of Pluto found that the high albedo of ices in SP causes cold-trapping of the volatile ices over timescales of millions of years[36]. Additionally, global circulation models involving the evolution of volatile ices (over timescales of thousands of years) show that these ices accumulate in the basin used to model SP[37].

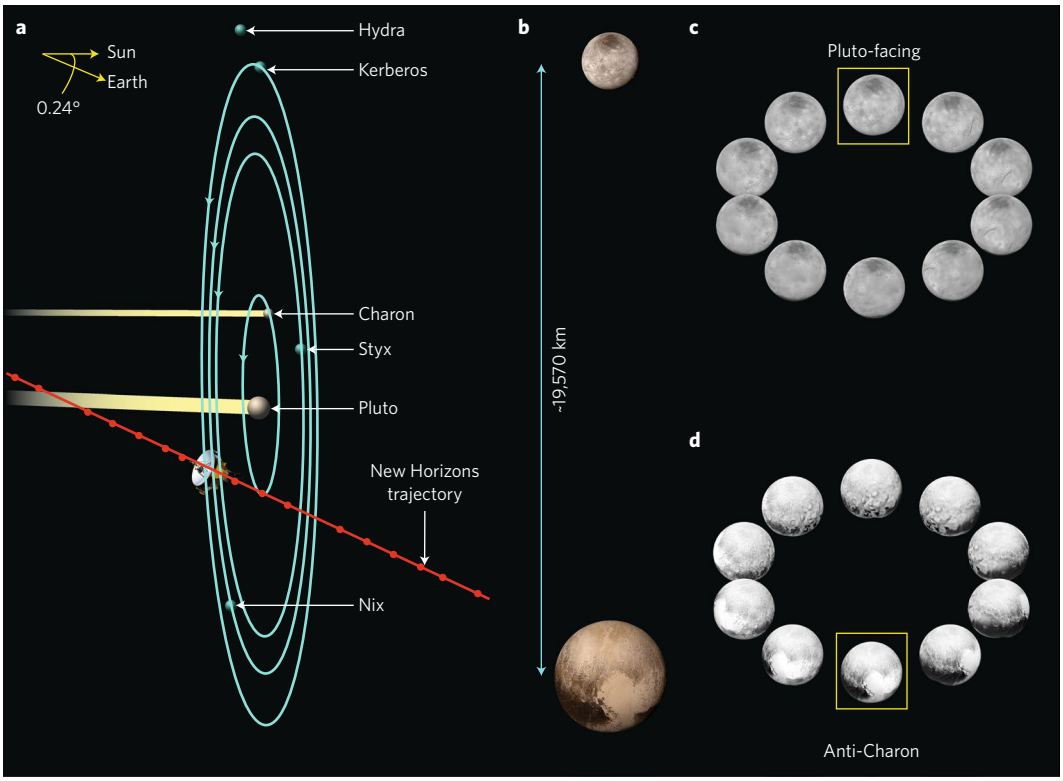

Fig. 2 | The dynamic duo. a, The 14 July 2015 encounter took the New Horizon spacecraft within ~12,500 km and ~27,000 km of Pluto's and Charon's surfaces, respectively. The exact geometry was constrained by the requirement that the spacecraft must pass through the shadows of both Pluto and Charon (indicated in yellow) to observe ultraviolet solar and radio science occultations of their atmospheres. **b**, Pluto and Charon observed in colour from a distance of ~250,000 km. Pluto and Charon are separated by ~19,570 kilometres (not shown to scale). **c**, Views of Charon based on New Horizons images taken over a ~6.4 day period (one rotation) as the spacecraft closed in from 10.2 million kilometres on 7 July 2015 to ~748,000 km on 13 July 2015. The area of Charon that was imaged at closest approach is the Pluto-facing hemisphere. The dark north pole is seen from all longitudes. **d**, Views of Pluto based on New Horizons images taken over the same period as in **c**. The hemisphere of Pluto that was visible from New Horizons at closest approach faces away from Charon. Panel **b** credit: NASA.

The latitudinal dependence of Pluto's composition (excluding SP, which is explained above) can be understood largely by the distribution of insolation over Pluto's surface (Fig. 5). Near the equator (Box 2) there is always some insolation over each Pluto day, resulting in long-term loss of volatile ices and thus leaving behind the dark equatorial band of non-volatile tholins. Pluto's north polar region has been experiencing summer with continuous insolation from 1987 to the current day. This intense insolation has caused sublimation of the most volatile of Pluto's ices (N_2) at the north pole, and atmospheric transport has redistributed the N_2 further south[34]. This can be seen in Fig. 4, where CH_4 is the most abundant species in the north.

While water ice was expected on Pluto's surface, it had not been identified in Earth-based spectroscopic observations[38]. Observations at higher spatial resolution by New Horizons allowed the identification and mapping of water ice on Pluto's surface for the first time. The signature of water ice is evident at mid- and equatorial-latitudes where volatile ices are depleted. The surface of Pluto's north pole is low in water ice and is instead dominated by methane ice, which sublimates and condenses through seasonal cycles of insolation to cover the non-volatile water ice. There are a number of mountain ranges at the western edge of SP. The surface composition of these mountains is more than 30% water ice. From the shape, location and composition of these mountains, they appear to be blocks of water ice crust that have broken off and travelled from the edge of SP. Because water ice is less dense than N_2 ice, it is possible that these mountains are floating on the glacial ices of SP.

Charon. In contrast, water ice is ubiquitous on Charon. Spectral features of water ice include the 1.65 μm band, which indicates that the water ice is in a crystalline form. Additionally, multiple sites exhibit an absorption feature at 2.1 μm, which is associated with ammonia hydrate. Local concentrations of ammonia hydrate are associated with some craters. Given that the destruction of ammonia ice by ultraviolet radiation takes ~10 Myr, these features are relatively young.

Unexpectedly, colour observations by New Horizons revealed that Charon's north pole is dark and red. Analysis of Charon's south pole (illuminated by sunlight reflected off Pluto) showed it was dark compared with the equatorial and mid-latitude regions, just like Charon's north pole. It is proposed that the red colouration is a result of tholins that accumulate each season[39]. CH_4 escapes Pluto's atmosphere at a rate of 5×10^{25} molecules s^{-1} (ref. [40]) and ~2.5% of this will intercept Charon. These CH_4 molecules will bounce around Charon's surface, where some will be cold-trapped at the winter poles. Irradiation by Lyα and cosmic rays over the long polar winter will convert the captured CH_4 to non-volatile, red tholin-like material, producing about 0.16 mm per million Earth years.

Pluto's cold and hazy atmosphere. In 1976, following the detection of methane ice on Pluto's surface, it was suggested that Pluto might have an atmosphere[41]. The first definitive observation of Pluto's atmosphere was from a stellar occultation[42] in 1988. As Pluto moved in front of the Galactic Plane as seen from the Earth in the 2000s, more occultation observations were made, with observations nearly

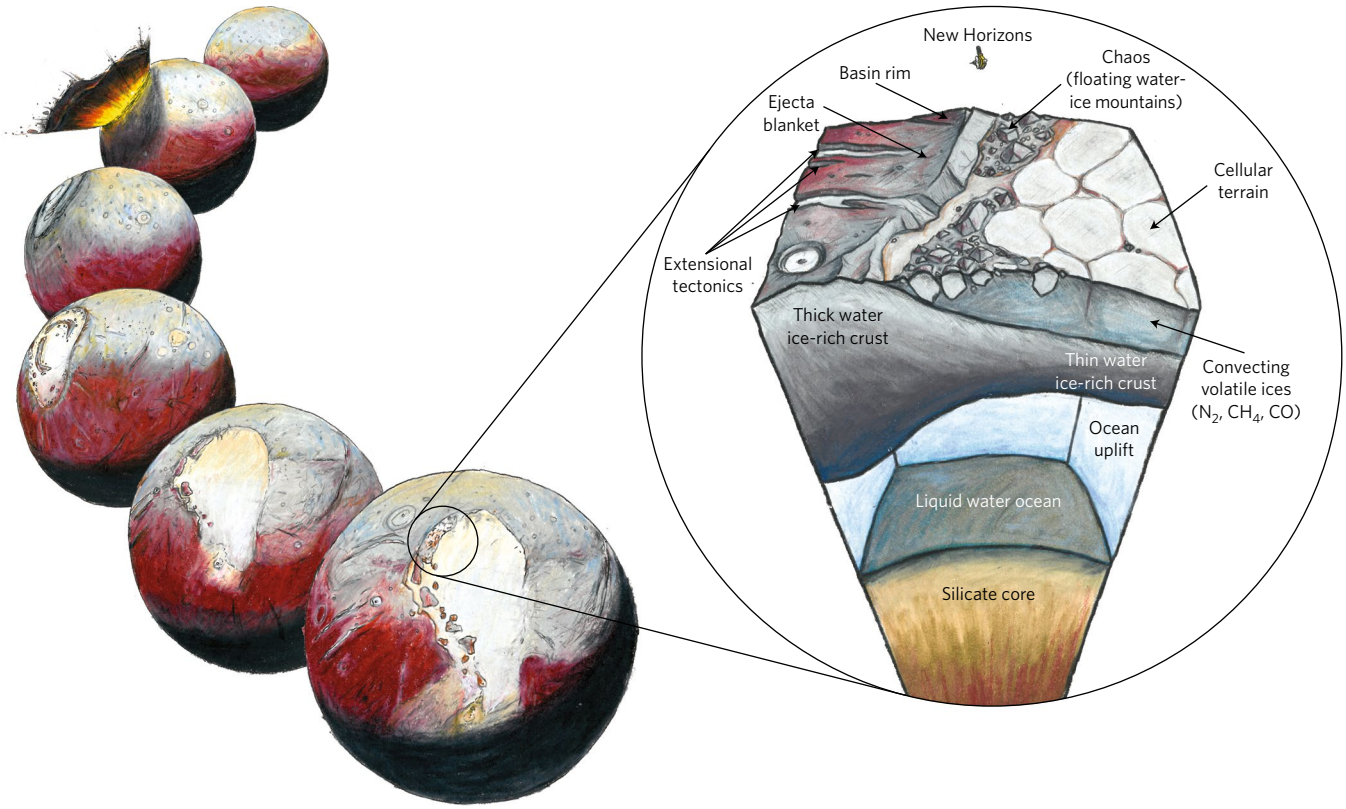

Fig. 3 | What lies beneath? a, The most striking feature on Pluto's anti-Charon hemisphere is SP, a large topographically low region filled with several kilometres of nitrogen, methane and carbon monoxide ices. In Pluto's past, this low region could have been the result of a large impactor[19]. **b**, The wide variety of surface features on the edges of SP, from extensional tectonics to possible cryovolcanoes, when combined with the surprising sphericity of Pluto and the unusual location of SP potentially due to re-orientation, paints a consistent picture that suggests Pluto's interior could harbour a subsurface liquid water ocean. Credit: James Keane.

every year over the period 2002–2016. Analysis of these observations demonstrated that Pluto's atmospheric pressure increased by a factor of two from 1988 to 2002 as Pluto receded from perihelion[43,44]. This may seem paradoxical because one might expect Pluto's atmosphere to be most dense at perihelion, where sunlight is the most intense, but it is explained by a high thermal inertia in Pluto's subsurface[45] that retains heat from perihelion. Later occultations showed that Pluto's atmospheric pressure has been continuing to increase with a tripling of atmospheric pressure from 1988 to 2015[46]. Ground-based spectroscopic observations provided the first direct detection of atmospheric gases with the detection of methane[47]. Later work detected CO and hydrogen cyanide[48] in Pluto's atmosphere.

New Horizons provided unique information about Pluto's atmosphere through ultraviolet solar and radio science occultations and high-phase-angle imaging. One surprising discovery was the blue haze layers encircling Pluto[40], which were observed after closest approach thanks to the strong forward-scattering properties of the haze particles. The haze extends to an altitude of >200 km with a scale height of 50 km (ref. [40]). The scattering and extinction properties of the haze suggest that the haze particles are fractal aggregates[40,49].

The composition of Pluto's atmosphere was measured by observing sunlight during a solar occultation. Different molecules absorbed the light at specific ultraviolet wavelengths in the range of 52–187 nm. This experiment provided the surprising result that the temperature in the upper atmosphere is much colder (69 K) than previously expected (~100 K; ref. [40]). The cooling mechanism is currently an open question. The observation of solar occultation also provided definitive detection of acetylene (C_2H_2), ethylene (C_2H_4) and ethane (C_2H_6), in addition to the expected N_2 (dominant species) and CH_4 (surface mixing ratio ~0.3%)[50]. The solar occultation data show a decrease in concentration of C_2 hydrocarbons below 200–400 km altitude, which is attributed to condensation[51].

Measurements of Pluto's surface pressure and temperature were made using an uplink radio science experiment, using four Deep Space Network stations to transmit a combination of right- and left-circularly polarized radiation through Pluto's atmosphere to New Horizons[52]. The radio science experiment was sensitive to the atmosphere in approximately the lowest 100 km altitude. Above ~20 km altitude, both the ingress and egress atmospheric profiles are consistent with each other and with stellar occultation observations[53]. Below ~20 km altitude, the ingress and egress temperature profiles differ significantly: the atmosphere is much warmer over the egress location (a dark area on the surface) than the ingress location (near the edge of SP)[53]. This is also reflected in the temperature gradients in the lowest 10 km: 6.4 K km^{-1} at ingress and 3.4 K km^{-1} at egress[53]. The mean surface pressure is 11.5 ± 0.7 μbar at a reference radius of 1,189.9 ± 0.2 km (ref. [53]).

Pluto's atmosphere should be considered in the context of other outer planet atmospheres, such as Triton and Titan. The main constituent in each of these three atmospheres is N_2, with methane as a minor constituent. The photochemistry in each of these atmospheres is expected to be similar, with ultraviolet radiation of methane producing hydrocarbons and ultraviolet radiation of N_2 producing ions, leading to haze[40]. The scattering properties of Pluto's haze particles are consistent with fractal aggregates, as on Titan[49]. All three atmospheres have haze layers, with the least haze

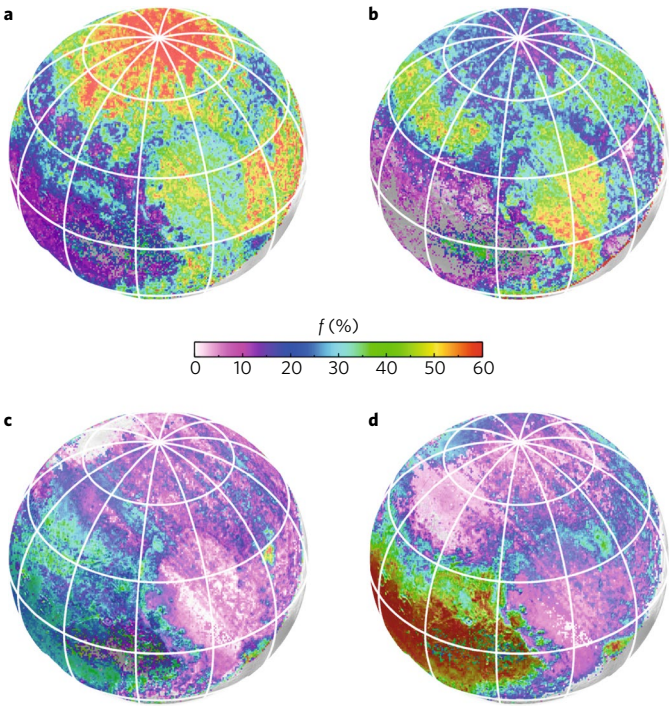

Fig. 4 | Composition maps of Pluto's surface from bidirectional reflectance modelling. a–d, Fractional abundances (*f*) of: CH_4-rich solid solution with <3% N_2 (**a**); N_2-rich solid solution with <5% CH_4 (**b**); H_2O ice (**c**); and tholin (**d**). Figure reproduced from ref. [33], Elsevier.

in Triton's atmosphere and the most opaque haze in Titan's. Triton and Pluto have tenuous atmospheres, with atmospheric pressures of the order of 10 μbar (Triton's atmospheric pressure was determined to be 14 μbar by Voyager 2 in 1989[54]), while Titan's is substantially thicker, with a pressure of ~1.5 bar. For comparison, the atmospheric pressure of 14 μbar occurs at ~400 km altitude on Titan. The atmospheric pressure of both Triton and Pluto has been observed to vary significantly with time.

New Horizons searched for an atmosphere around Charon, but no evidence of an atmosphere was found[55].

Open questions

The historic July 2015 flyby provided new insights into the Pluto system. We are inspired to ask new questions, thanks to the discovery of glaciers composed of N_2, CH_4 and CO flowing on Pluto, mountains of water ice, a global blue atmosphere with haze and evidence suggestive of a subsurface ocean. More laboratory studies are needed to better understand the Pluto system and other cold distant Kuiper Belt objects. Experiments to better understand the rheology of Pluto's volatile ices (such as flow rates, stain and stress parameters) are needed. Furthermore, measurements of the visible and near-infrared optical constants of ice mixtures such as N_2, CH_4 and CO are needed to help improve reflectance models. Additionally, ultraviolet optical constants are needed at low temperatures for the C_2 hydrocarbons seen in Pluto's atmosphere.

Pluto and its moons have now returned to the realm of astronomy. Pluto is only a few pixels across when imaged through the soon-to-be launched James Webb Space Telescope (JWST), yet JWST's unprecedented spectral sensitivity and factor of approximately

Box 2 | Seasons and insolation

Pluto experiences complex seasonal variation across a number of different timescales. Owing to Pluto's eccentric orbit, insolation at aphelion (49 au) is 2.6 times lower than that at perihelion (29 au) over the course of its 248 year orbit. Due to Pluto's large obliquity (~120°), its polar regions experience extended periods of arctic night. Pluto's obliquity is not constant: it precesses with a peak-to-peak amplitude of 23° over ~3 Myr. When considering these effects on Pluto and Charon, latitudes between 13° N and 13° S always receive sunlight during a diurnal cycle (6.4 days), latitudes poleward of 38° experience arctic seasons every Pluto year, and latitudes poleward of 77° never have the sun directly overhead[63]. These longitudinal regions show a correlation with albedo and composition (Fig. 5).

On even longer timescales (~3.7 Myr), Pluto's orbital longitude of perihelion regresses. The combination of all these affects results in epochs of extreme seasons[36]. An example of this was 0.9 Myr ago, when Pluto's subsolar point at perihelion was at high northern latitude, resulting in a short but intense artic summer[36].

Models of atmospheric pressure, given the obliquity precession and orbital variations, predict possible high pressures (as much as hundreds of millibars, depending on assumptions of polar albedo), which could explain geomorphic features that suggest possible previous liquids on the surface of Pluto, like the dendritic terrain and lake-like features near the edge of SP[64].

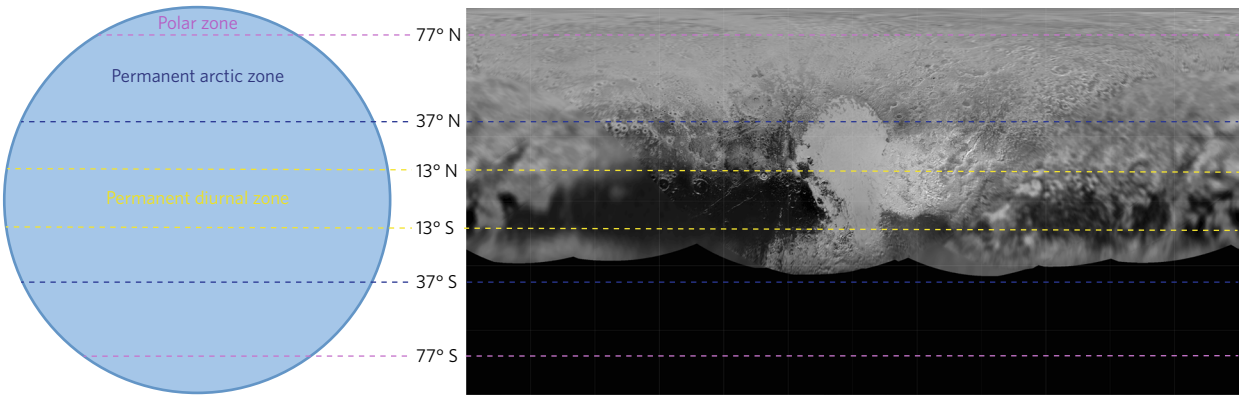

Fig. 5 | Pluto's climate regions. Longitudinal regions related to solar insolation and seasons show a correlation with albedo and composition. Figure adapted from ref. [63], Elsevier.

six improvement in spectral resolution compared with New Horizons will allow for the detection of new species and regular measurement of Pluto's surface ices. NASA's airborne Stratospheric Observatory for Infrared Astronomy can be utilized in combination with JWST and ground-based telescopes to monitor Pluto's evolving atmosphere via occultation events. Continued monitoring of Pluto's hemispherical surface composition with ground-based near-infrared telescopes and the Atacama Large Millimeter/submillimeter Array observatory, which can also probe its atmosphere down to altitudes of several hundred kilometres, are all important parts in this next chapter of understanding the Pluto system.

Received: 21 June 2017; Accepted: 14 August 2017;
Published online: 25 September 2017

References

1. Buratti, B. et al. Photometry of Pluto in the last decade and before: evidence for volatile transport? *Icarus* **162**, 171–182 (2003).
2. Buratti, B. et al. Photometry of Pluto 2008–2014: evidence of ongoing seasonal volatile transport and activity. *Astrophys. J. Lett.* **804**, L6–L12 (2015).
3. Buie, M. W. et al. Pluto and Charon with the Hubble Space Telescope. II. Resolving changes on Pluto's surface and a map for Charon. *Astron. J.* **139**, 1128–1143 (2010).
4. Buie, M. W. & Tholen, D. J. The surface albedo distribution of Pluto. *Icarus* **79**, 23–37 (1989).
5. Buie, M. W. et al. in *Pluto and Charon* (eds Stern, S. A. & Tholen, D. J.) 269–293 (Univ. Arizona Press, Tucson, Arizona, 1997).
6. Tholen, D. J. & Buie, M. W. in *Pluto and Charon* (eds Stern, S. A. & Tholen, D. J.) 347–390 (Univ. Arizona Press, Tucson, Arizona, 1997).
7. Lellouch, E. et al. Pluto's lower atmosphere structure and methane abundance from high-resolution spectroscopy and stellar occultations. *Astron. Astrophys.* **495**, L17–L21 (2009).
8. Buie, M. W., Tholen, D. J. & Horne, K. Albedo maps of Pluto and Charon: initial mutual events results. *Icarus* **97**, 211–227 (1992).
9. Young, E. F. et al. Mapping the variegated surface of Pluto. *Astron. J.* **117**, 1063–1076 (1999).
10. Young, E. F., Binzel, R. P. & Crane, K. A two-color map of Pluto's sub-Charon hemisphere. *Astron. J.* **121**, 552–561 (2001).
11. Binzel, R. P. Hemispherical color differences on Pluto and Charon. *Science* **241**, 1070–1072 (1988).
12. Albrecht, R. et al. High-resolution imaging of the Pluto–Charon system with the Faint Object Camera of the Hubble Space Telescope. *Astrophys. J.* **435**, L75–L78 (1994).
13. Stern, S. A., Buie, M. W. & Trafton, L. M. HST high-resolution images and maps of Pluto. *Astron. J.* **113**, 827–843 (1997).
14. Young, L. A. et al. New Horizons: anticipated scientific investigations at the Pluto system. *Space Sci. Rev.* **140**, 93–127 (2008).
15. Buratti, B. et al. Global albedos of Pluto and Charon from LORRI New Horizons observations. *Icarus* **287**, 207–217 (2017).
16. Moore, J. M. et al. The geology of Pluto and Charon through the eyes of New Horizons. *Science* **351**, 1284–1293 (2016).
17. Hammond, N. P., Barr, A. C. & Parmentier, E. M. Recent tectonic activity on Pluto driven by phase changes in the ice shell. *Geophys. Res. Lett.* **43**, 6775–6782 (2016).
18. Howard, A. D. et al. Pluto: pits and mantles on uplands north and east of Sputnik Planitia. *Icarus* **293**, 218–230 (2017).
19. Johnson, B. C. et al. Formation of the Sputnik Planum basin and the thickness of Pluto's subsurface ocean. *Geophys. Res. Lett.* **43**, 10068–10077 (2016).
20. McKinnon, W. B. et al. Convection in a volatile nitrogen-rich-ice layer drives Pluto's geologic vigour. *Nature* **534**, 82–85 (2016).
21. White, O. L. et al. Geologic mapping of Sputnik Planitia on Pluto. *Icarus* **287**, 261–286 (2017).
22. Hamilton, D. P. et al. The rapid formation of Sputnik Planitia early in Pluto's history. *Nature* **540**, 97–99 (2016).
23. Nimmo, F. et al. Global mean radius and shape of Pluto and Charon from New Horizons images. *Icarus* **287**, 12–29 (2017).
24. Schenk, P. M. & Zahnle, K. On the negligible surface age of Triton. *Icarus* **192**, 135–149 (2007).
25. Nimmo, F. & Spencer, J. R. Powering Triton's recent geological activity by obliquity tides: implications for Pluto geology. *Icarus* **246**, 2–10 (2015).
26. Beyer, R. A. et al. Charon tectonics. *Icarus* **287**, 161–174 (2017).
27. Robbins, S. et al. Craters in the Pluto–Charon system. *Icarus* **287**, 187–206 (2017).
28. Stern, S. A. et al. The Pluto system: initial results from its exploration by New Horizons. *Science* **350**, 1815 (2015).
29. Rhoden, A. R. et al. The interior and orbital evolution of Charon as preserved in its geologic record. *Icarus* **246**, 11–20 (2015).
30. Grundy, W. M. et al. Near-infrared spectral monitoring of Pluto's ices: spatial distribution and secular evolution. *Icarus* **223**, 710–721 (2013).
31. Prokhvatilov, A. I. & Yantsevich, L. D. X-ray investigation of the equilibrium phase diagram of CH_4–N_2 solid mixtures. *Sov. J. Low Temp. Phys.* **9**, 94–98 (1983).
32. Grundy, W. M. et al. Surface compositions across Pluto and Charon. *Science* **351**, aad9189 (2016).
33. Protopapa, S. et al. Pluto's global surface composition through pixel-by-pixel Hapke modeling of New Horizons Ralph/LEISA data. *Icarus* **287**, 218–228 (2017).
34. Schmitt, B. et al. Physical state and distribution of materials at the surface of Pluto from New Horizons LEISA imaging spectrometer. *Icarus* **287**, 229–260 (2017).
35. Cruikshank, D. P., Imanaka, H. & Dalle Ore, C. M. Tholins as coloring agents on outer solar system bodies. *Adv. Space Res.* **36**, 178–183 (2005).
36. Earle, A. et al. Long-term surface temperature modeling of Pluto. *Icarus* **287**, 37–46 (2017).
37. Bertrand, T. & Forget, F. Observed glacier and volatile distribution on Pluto from atmosphere–topography processes. *Nature* **540**, 86–89 (2016).
38. Cruikshank, D. et al. The surface compositions of Pluto and Charon. *Icarus* **246**, 82–92 (2015).
39. Grundy, W. M. et al. The formation of Charon's red poles from seasonally cold-trapped volatiles. *Nature* **539**, 65–68 (2016).
40. Gladstone, G. R. et al. The atmosphere of Pluto as observed by New Horizons. *Science* **351**, aad8866 (2016).
41. Cruikshank, D. P. et al. Pluto — evidence for methane frost. *Science* **194**, 835–837 (1976).
42. Elliot, J. L. et al. Pluto's atmosphere. *Icarus* **77**, 148–170 (1989).
43. Elliot, J. L. et al. The recent expansion of Pluto's atmosphere. *Nature* **424**, 165–168 (2003).
44. Sicardy, B. et al. Large changes in Pluto's atmosphere as revealed by recent stellar occultations. *Nature* **424**, 168–170 (2003).
45. Olkin, C. B. et al. Evidence that Pluto's Atmosphere does not collapse from occultations including the 2013 May 04 event. *Icarus* **246**, 220–225 (2015).
46. Sicardy, B. et al. Pluto's atmosphere from the 29 June 2015 ground-based stellar occultation at the time of the New Horizons' flyby. *Astrophys. J. Lett.* **426**, 220–225 (2016).
47. Young, L. A. et al. Detection of gaseous methane on Pluto. *Icarus* **127**, 258–262 (1997).
48. Lellouch, E. et al. Detection of CO and HCN in Pluto's atmosphere with ALMA. *Icarus* **286**, 289–307 (2017).
49. Gao, P. et al. Constraints on the microphysics of Pluto's photochemical haze from New Horizons observations. *Icarus* **287**, 116–123 (2017).
50. Young, L. A. et al. Structure and composition of Pluto's atmosphere from the New Horizons solar ultraviolet occultation. *Icarus* https://doi.org/10.1016/j.icarus.2017.09.006 (2017).
51. Wong, M. L. et al. The photochemistry of Pluto's atmosphere as illuminated by New Horizons. *Icarus* **287**, 110–115 (2017).
52. Sepan, R. et al. Preparing and implementing the New Horizons uplink occultations: applying concepts, tools, and lessons learned over nearly a decade of flight to achieve a successful operation. *SpaceOps 2016 Conf.* AIAA 2016–2537 (2016).
53. Hinson, D. P. et al. Radio occultation measurements of Pluto's neutral atmosphere with New Horizons. *Icarus* **290**, 96–111 (2017).
54. Gurrola, E. M. *Interpretation of Radar Data from the Icy Galilean Satellites and Triton*. PhD thesis, Stanford Univ. (1995).
55. Stern, A. S. et al. New Horizons constraints on Charon's present day atmosphere. *Icarus* **287**, 124–130 (2017).
56. Tombaugh, C. W. Reminiscences of the discovery of Pluto. *Sky & Telescope* 264–270 (March 1960).
57. Christy, J. W. & Harrington, R. S. The satellite of Pluto. *Astron. J.* **83**, 1005–1008 (1978).
58. Christy, J. W. & Harrington, R. S. The discovery and orbit of Charon. *Icarus* **44**, 38–40 (1980).
59. Weaver, H. A. et al. Discovery of two new satellites of Pluto. *Nature* **439**, 943–945 (2006).
60. Showalter, M. R. et al. New satellite of (134340) Pluto: S/2011 (134340). *Int. Astron. Union Circ.* 9221 (2011).
61. Showalter, M. R. et al. New satellite of (134340) Pluto: S/2012 (134340). *Int. Astron. Union Circ.* 9253 (2012).
62. Weaver, H. A. et al. The small satellites of Pluto as observed by New Horizons. *Science* **351**, 1281 (2016).
63. Binzel, R. P. et al. Climate zones on Pluto and Charon. *Icarus* **287**, 30–36 (2017).
64. Stern, S. A. et al. Past epochs of significantly higher pressure atmospheres on Pluto. *Icarus* **287**, 47–53 (2017).

Acknowledgements
This work was supported by the NASA New Horizons project. We thank the engineers and staff of the New Horizons team whose dedication enabled the initial reconnaissance of the Pluto system.

Author contributions
C.B.O. wrote Box 2 and the sections on surface composition and atmospheres. K.E. wrote Box 1 and sections entitled 'Light curves to maps' and 'Open questions.' J.S. detailed the geology of Pluto and Charon.

Competing interests
The authors declare no competing financial interests.

Additional information
Reprints and permissions information is available at www.nature.com/reprints.

Correspondence and requests for materials should be addressed to C.B.O.

Publisher's note: Springer Nature remains neutral with regard to jurisdictional claims in published maps and institutional affiliations.